Civil Engineering Infrastructures Journal xx,xx
DOI: 10.22059/ceij.2025.374673.2041

**TECHNICAL NOTES**

# Double Fourier Series Method for Bending Solutions of Simply Supported Mindlin Plates

**Charles Chinwuba Ike**

Department of Civil Engineering, Enugu State University of Science and Technology, Agbani, 402004, Enugu State, Nigeria

Received: 03/04/2024
Revised: 11/10/2024
Accepted: 07/11/2024

**Abstract**
This study presents first principles derivation of the partial differential equations (PDEs) for flexural solutions of Mindlin's first order shear deformation plate theory (MFSDPT). The PDEs were formulated using the kinematics, constitutive and equilibrium equations in an equilibrium approach. The resulting PDEs are coupled system of three PDEs in three unknown displacements – one transverse displacement $w$ and two rotations $\lambda_x$ and $\lambda_y$. The study considered a simply supported thick plate bending problem for illustrative solutions. Double finite sine transformation methodology (DFSTM) was utilized for solutions in that double sine kernel functions of the transformation satisfies the simply supported boundary conditions. The DFSTM simplified the system of PDEs to a system of three algebraic equations with displacement amplitudes $W_{mn}$, $A_{mn}$ and $B_{mn}$ for $w$, $\lambda_x$ and $\lambda_y$ respectively. Analytical solutions were obtained for uniformly and linearly distributed loadings transversely applied on the domain. The present results for in-plane and transverse displacements are comparable to previously obtained results. The MFSDPT results are closed form in the theoretical framing of small displacement elasticity theory for homogeneous, isotropic thick plates. The DFSTM has been shown to give accurate solutions to the resulting equations.

**Keywords:** Mindlin plate, first order shear deformation plate theory, double finite sine transform method, integral transform, differential equation of equilibrium

## 1. Introduction

Plates are load transmitting structures used in naval, aeronautical, spacecraft, building, machine and civil structures. They are known to have in-plane dimensions that are much larger than their transverse dimensions. The in-plane dimensions are length and breadth while the transverse dimension is the depth, *h*. They can be subjected to static, dynamic or in-plane compressive forces. Depending on their natural properties, they can be isotropic, anisotropic, orthotropic; homogenous or non-homogenous. When made of different materials, they are called composite plates (Pagano, 1970). They can also be made of laminae and hence become laminated plates. They can be of different shapes – rectangular, skewed, circular, trapezoidal, rhombic, or polygonal.

The behaviour of plates is largely determined by the ratios of the least in-plane dimension to the thickness, *h*. Plates are called thin when the ratio of the thickness to the width is less than 0.05; called moderately thick when this ratio exceeds 0.05 but less than 0.1; and thick when the ratio exceeds 0.20.

Commonly, thin plates have ratios of width (*a*) to thickness (*h*) lying between 8 and 100. Thick plates have $a/h \leq 10$. When the ratio of depth to breadth is greater than 0.10, the use of thick plate theories become imperative because it becomes thick.

Kirchhoff (1850) derived Kirchhoff plate theory (KPT) for plates bending using the Navier-Kirchhoff hypotheses requiring rectilinear lines originally orthogonal to the plate's middle surface remaining rectilinear and orthogonal to the plate's mid surface after flexural deformations, and also remains unstretched (Alcybeev et al, 2022; Goloskokov and Matrosov, 2022; Singhatandgid and Singhanart, 2019).

The Navier-Kirchhoff orthogonality assumptions imply that transverse shear deformation effects are neglected in the formulation, thus restricting validity for resulting theory to slender plates where transverse shearing deformation effects do not significantly affect the flexural or buckling behaviours (Ike, 2022; Mama et al, 2020). KPT gives a fourth order partial differential equation in terms of the transverse displacement, and has been solved using several methods yielding good results for thin plate bending, but unsatisfactory results for moderately thick and thick plates.

Classical plate bending theory (CPBT) is one of the oldest theories used for plate bending solutions. The CPBT equations exclude transverse shear deformation effects and this limits it to thin plates. It has been observed that CPBT underestimates the deflection of thick plates, rendering it unsafe for use in thick plate bending analysis. The CPBT also gives overestimated values for natural vibration frequencies and stability loads when applied to moderately thick plates. The errors of the CPBT when used for thick plate analysis increase with increase in the plate thickness. The drawbacks of the CPBT have resulted in the search for refined, sinusoidal, hyperbolic and parabolic plate theories for the analysis of moderately thick plates.

Several researchers have formulated other theories that consider transverse shearing deformation effects on bending and buckling solutions of plates. The effects of transverse shear deformation is significant for the flexural and stability solutions of moderately thick and thick plates.

The formulations of the first order shear deformable plate theories involve the introduction of transverse shear correction coefficient. The shear correction coefficient is required in order to correct the transverse shear stresses obtained by Mindlin's FOSDPT. This is because the FOSDPT yields constant values of transverse shearing stresses across the plate depth, rather than parabolic or quadratic transverse shearing stresses distribution obtained using classical mathematics theories of elasticity. The fact that transverse shear stress-free boundary conditions are violated in the FOSDPT has been considered to be a serious limitation of FOSDPTs.

However, transverse shear stress correction coefficients ameliorate the discrepancies obtained in the FOSDPT estimation of transverse shear forces and the elasticity solutions. Extensive research works have been presented for issues of determinations use of transverse shearing stress correction parametres.

Mindlin (1951) used a displacement based procedure to derive another theory called Mindlin plate theory (MiPT), another first order shear deformable plate theory. The GPDE are represented by three equations, with three unknown displacements – two rotations and one transverse deflections.

In MiPT, the transverse shear stress at the plate surfaces $(z = \pm 0.5h)$ are constant and hence violate the transverse shear stress free boundary conditions at the plate surfaces. In order to overcome this defect, transverse shear stress correction factors were defined in order to ensure the prediction of correct strain energy of deformation.

Nwoji et al (2018) studied the bending solutions of simply supported rectangular Mindlin plates under bisinusoidal transverse loading covering the plate. They obtained closed form analytical solutions that satisfied the PDEs of equilibrium at every points, and also satisfied simple support boundary conditions. Their solutions agreed with previous solutions in literature.

Despite its amelioration by the shear correction factors, the violation of the transverse shear stress-free boundary conditions of the surfaces $(z = \pm 0.5h)$ is the major defect of the MiPT. In addition, there is a lack of systematic procedure for calculating the transverse shear stress correction factors in FOSDPT.

Mindlin plate theoretical frameworks are basically simple to use for modeling the shear deformation behaviour of thick plates. Research efforts to further improve on the FOSDPTs by obviating the need for transverse shear stresses correction factors have led to the development of transverse shear deformable plate theories (SDPTs), Higher order shear deformation plate theories (HOSDPTs) and Refined shear deformation plate theories (RefSDPTs).

SDPTs were studied by Ghugal and Pawar (2011). Ghugal and Pawar (2011) used hyperbolic shear deformable plate theoretical framework for the flexural and buckling solutions of thick plates, respectively. Ghugal and Sayyad (2013) also presented TSDPT for the bending solutions of thick orthotropic plates. Sayyad (2013) used exponential shear deformable plate theories (ESDPT) for the bending solutions of thick non-isotropic plates.

HOSDPTs were investigated by Reddy (2004). Refined shear deformable plate theories (RefSDPTs) were derived and implemented by Do et al (2020) and Rouzegar and Abdoli Sharifpoor (2015).

Thick plates problems were formulated and solved using exact methods of the theory of elasticity by Pagano (1970). Finite difference method (FDM) has been utilized for approximate analysis of plate problems by Pisacic et al (2019).

Onyeka et al (2023) explored a polynomial displacement function in a potential energy methodology to find bending solutions for thick plate with simply supported, free and clamped (SCFS) edges. They obtained solutions for center deflections that were 2.9% – 3.7% different from the exact solutions of three dimensional (3D) elasticity theory.

Onyeka et al (2022) used an energy minimization methodology for bending solutions of thick rectangular clamped plates. They used 3D kinematic and constitutive relations and shear correction factors were not needed in their equations. They used a trigonometric displacement function to obtain satisfactory results that differed from the Mindlin plate solution by 3.02% and differed from the HSDPT (using polynomial displacement function) by 0.33%.

Gajbhiye et al (2021) used a fifth order shear deformable theoretical framework for free vibration solutions of thick isotropic plate, but didn't consider the use for flexural analysis. In another study, Gajbhiye et al (2022) explored a quasi-three-dimensional theoretical formulation considering transverse shearing and normal deformations for obtaining flexural solutions of simply supported sandwich plates. Their work did not need transverse shearing stress modification factors and satisfied the transverse shear-stress free boundary conditions at the plate surfaces. They utilized virtual work principle for obtaining the domain equations of equilibrium and the boundary conditions, and Navier's single series method to obtain accurate solutions for sinusoidal and uniformly distributed transverse loadings.

Zhong and Xu (2017) studied analytical flexural problems of rectangular thick plates with clamped edges. The thick plate was modelled using Mindlin plate theory. They introduced a new function that was used to decouple the three coupled equations of the plate into three independent uncoupled PDEs that could be solved separately.

Do et al (2020) developed a single displacement variable refinement of plate theory for the flexural solutions of functionally graded material (FGM) plates. They used a displacement method and equilibrium approach to find field equations that did not need shear correction factors. They applied Navier's series methodology for obtaining accurate bending solutions for simply supported plates.

Rouzeger and Abdoli Sharifpoor (2015) implemented a finite element method using the two-displacement variables refinements of plate theory (RefPT) for the bending solutions of plates. The RefPT used is applicable to slender plates and to thick plates and yields quadratic variations of transverse shear stresses across the depth, thus satisfying the transverse shear-stress free boundary conditions at the plate surfaces $(z = \pm 0.5h)$

Onah et al (2020) have formulated using rigorous first principles methods displacements and stress functions for three dimensional analysis of elastostatic flexural problems, and illustrated their applications for accurate bending solutions of thick circular plates under transverse uniformly distributed load.

Recently, Ike (2023) presented third order shear deformable plate flexural formulations for moderately thick and thick plates. The formulation used a third order polynomial function of the transverse coordinate, made to satisfy the 3D strain-displacement relations of elasticity theory and the transverse shear stress-free boundary conditions at $z = \pm 0.5h$. The formulations used variational calculus methods for deriving system of domain equations which were coupled and contained three unknowns. The set of coupled equations was solved for various loading cases using Navier's series method. Exact solutions were obtained in the study as all boundary conditions were satisfied together with the governing PDEs.

Haggblad and Bathe (1990) investigated plate bending finite elements derived via Ressner Mindlin plate theories (RMPTs). Their work provided insight and guidance on how to choose boundary conditions in the RMPT based finite elements. Belounar et al (2020) developed novel triangular finite elements for the natural dynamics analysis for plates. They used the RMPT and strain-based formulation; and used three displacement degrees of freedom at each of the three corner nodes. The element was based on a linear variation of the three bending strains and constant transverse shear strains. The element was found to give accurate results for moderately thick plates.

Shahnavaz et al (2023) derived accurate solutions for the freely vibrating in-plane FGM plates using displacement-based FEM by using accurate shape functions that interpolate the displacement field inside the element. Their work however did not consider static bending analysis.

Altekin (2018) studied RMPT in the analysis of thick elliptical shaped plates under transverse load by the use of four-noded isoparametric quadrilateral plate bending elements having three degrees of freedom per node. Parameter based studies in their work showed that the results agreed with previous results.

Zhong and Xu (2017) studied flexural analysis of rectangular thick plate with various combinations of clamped and supported edges. They used Mindlin's higher-order shear deformation plate theory. They used novel functions to uncouple the three coupled PDEs of the domain, thus rendering them solvable independently. They solved the uncoupled equations to obtain closed form solutions for clamped and supported edges. Shetty et al (2022) developed a third order one-displacement variable plate model for "bending analysis of thick plates with simply supported edges". The merit of their formulation is that the domain equation and expressions for internal forces are analogous to those of thin plates bending theories equations. Other significant studies on plates include: Yekani and Fallah (2020); Belounar et al (2020) and Kianmofrad et al (2018).

Literature review shows that there are few studies on the flexural vibrations of thick plates modeled using Mindlin plate theoretical frameworks and focused on a first principles systematic derivation of the governing domain equations. Still very few studies have focused on providing solutions to the Mindlin plate equations for bending of thick plates under uniform and linear distributed transverse loadings.

In this paper, thick plate flexure analysis problems are modeled via Mindlin plate theory derived rigorously using Newtonian equilibrium methods, and the fundamental principles of small displacement elasticity theory in three dimensions. The governing equations of equilibrium derived are solved using double Fourier series method for the case of simply supported plate boundaries and the two cases of transversely applied:

- uniform loads, and
- linear distribution of loadings.

## 2. Theoretical Framework

### 2.1 Assumptions

The assumptions are as follows:

(i) The plate material is linear in its elastic properties. It is also isotropic and homogeneous.

(ii) The displacement variation across the thickness is linear, yielding constant transverse shear strains and transverse shear stresses across the depth.

(iii) A small line segment initially orthogonal to the plate middle surface would remain rectilinear. However it will not remain normal to the plate middle surface after deformation.

(iv) The plate is transversely inextensible.

### 2.2 Thick plate bending problem

This work considers a simply supported moderately thick plate bending problem depicted in Figure 1 defined by the three-dimensional Cartesian coordinates $x$, $y$, $z$ by:

$$0 \le x \le a, \quad 0 \le y \le b, \quad -0.5h \le z \le 0.5h;$$

where $a$ and $b$ are in-plane dimensions of the plate and $h$ is depth of the plate.

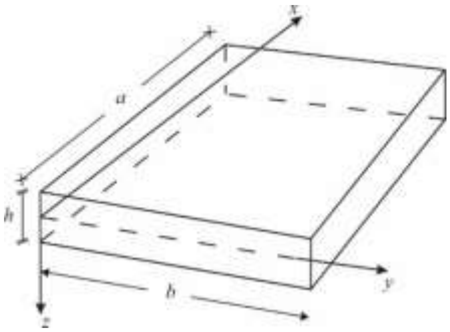


Figure 1: Isometric view of rectangular thick plate

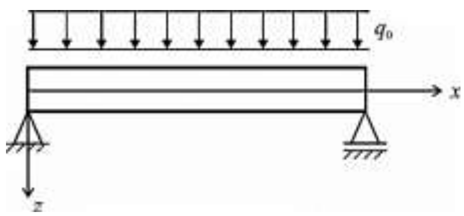


Figure 2: Cross-sectional view of simply supported thick rectangular plate under uniformly distributed load, $q_0$

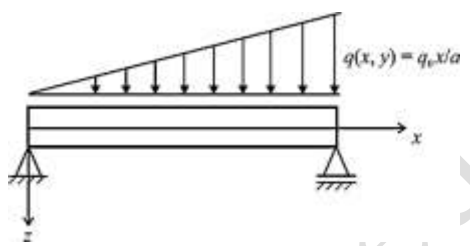


Figure 3: Cross-sectional view of simply supported thick rectangular plate under linear load distribution $q_z(x, y) = q_0 x / a$

### 2.3 Displacement field

The displacement expressed using transverse displacement of the middle surface $w(x, y, z = 0)$ and the rotations $\lambda_x$ and $\lambda_y$ of the middle surface. At a generic point $(x, y, z)$ on the plate, displacement field components are:

$$u = z\lambda_x \tag{1a}$$

$$v = \lambda_y \tag{1b}$$

$$w = w \tag{1c}$$

$u$, $v$, $w$ are the displacement field components in the $x$, $y$, and $z$ coordinates respectively. The in-plane displacement components $u(x, y, 0)$ and $v(x, y, 0)$ vary linearly with the thickness coordinate variable, $z$, rendering the resulting formulation FOSDPT.

### 2.4 Strain fields

The strain fields are found from unknown displacements field by substituting displacement fields in the kinematic relations of small displacement elasticity theory. Thus normal strains $\varepsilon_{xx}$, $\varepsilon_{yy}$, $\varepsilon_{zz}$ are found as: The formulation does not extend to large deflection analysis and geometrically nonlinear problems.

$$\varepsilon_{xx} = z\frac{\partial \lambda_x}{\partial x} \tag{2a}$$

$$\varepsilon_{yy} = z\frac{\partial \lambda_y}{\partial y} \tag{2b}$$

$$\varepsilon_{zz} = z\frac{\partial w}{\partial z} = 0 \tag{2c}$$

The shear stains $\gamma_{xy}$, $\gamma_{yz}$ and $\gamma_{xz}$ are found as:

$$\gamma_{xy} = z\left(\frac{\partial \lambda_x}{\partial y} + \frac{\partial \lambda_y}{\partial x}\right) \tag{2d}$$

$$\gamma_{xz} = \lambda_x + \frac{\partial w}{\partial x} \tag{2e}$$

$$\gamma_{yz} = \lambda_y + \frac{\partial w}{\partial y} \tag{2f}$$

### 2.5 Stress-strain law

The stress-strain relations for homogeneous isotropic linear elastic thick plate material are used in this paper. The formulation does not apply to anisotropic, non-homogeneous plates.

### 2.6 Stress-displacement equations

The stress-displacement relations are found from stress-strain and strain-displacements equations as:

$$\sigma_{xx} = \frac{Ez}{1-\mu^2}\left(\frac{\partial \lambda_x}{\partial x} + \mu\frac{\partial \lambda_y}{\partial y}\right) \tag{3a}$$

$$\sigma_{yy} = \frac{Ez}{1-\mu^2}\left(\mu\frac{\partial \lambda_x}{\partial x} + \frac{\partial \lambda_y}{\partial y}\right) \tag{3b}$$

$$\tau_{xy} = Gz\left(\frac{\partial\lambda_x}{\partial y} + \frac{\partial\lambda_y}{\partial x}\right) \quad (3c)$$

$$\tau_{xz} = G\left(\lambda_x + \frac{\partial w}{\partial x}\right) \quad (3d)$$

$$\tau_{yz} = G\left(\lambda_y + \frac{\partial w}{\partial y}\right) \quad (3e)$$

$G$ is the shear modulus, $E$ is the Young's modulus, $\mu$ is the Poisson's ratio.

Equations (3d) and (3e) reveal that $\tau_{xz}$ and $\tau_{yz}$ are constant across the plate thickness and hence transverse shear stress-free boundary conditions at the plate surfaces are violated. However, shear stress correction factors are introduced to ensure that the correct shearing forces are obtained in this formulation.

## 2.7 Internal force resultants

The distribution of bending moments $M_{xx}$, $M_{yy}$ and twisting moments $M_{xy}$ are given by integrals across the thickness:

$$M_{xx} = \int_{-h/2}^{h/2} \sigma_{xx} z\,dz \quad (4a)$$

$$M_{yy} = \int_{-h/2}^{h/2} \sigma_{yy} z\,dz \quad (4b)$$

$$M_{xy} = \int_{-h/2}^{h/2} \tau_{xy} z\,dz \quad (4c)$$

The shear force distributions $Q_x$ and $Q_y$ are given by:

$$Q_x = \int_{-h/2}^{h/2} k_s \tau_{xz}\,dz \quad (4d)$$

$$Q_y = \int_{-h/2}^{h/2} k_s \tau_{yz}\,dz \quad (4e)$$

where $k_s$ is the transverse shearing stress correction factor.

By substitution of the expressions for stresses and integration, the internal force resultants are obtained as:

$$M_{xx} = D\left(\frac{\partial\lambda_x}{\partial x} + \mu\frac{\partial\lambda_y}{\partial y}\right) \quad (5a)$$

$$M_{yy} = D\left(\mu\frac{\partial\lambda_x}{\partial x} + \frac{\partial\lambda_y}{\partial y}\right) \quad (5b)$$

$$M_{xy} = \frac{D(1-\mu)}{2}\left(\frac{\partial\lambda_x}{\partial y} + \frac{\partial\lambda_y}{\partial x}\right) \quad (5c)$$

$$Q_x = k_s Gh\left(\lambda_x + \frac{\partial w}{\partial x}\right) \quad (5d)$$

$$Q_y = k_s Gh\left(\lambda_y + \frac{\partial w}{\partial y}\right) \quad (5e)$$

## 2.8 Partial Differential Equations of Static Equilibrium

The PDEs of static equilibrium are expressed using force resultants as:

$$Q_x = \frac{\partial M_{xx}}{\partial x} + \frac{\partial M_{xy}}{\partial y} \quad (6a)$$

$$Q_y = \frac{\partial M_{xy}}{\partial x} + \frac{\partial M_{yy}}{\partial y} \quad (6b)$$

$$\frac{\partial Q_x}{\partial x} + \frac{\partial Q_y}{\partial y} + q_z(x,y) = 0 \quad (6c)$$

Substitution of Equations (6a) and (b) into Equation (6c) gives, after simplification:

$$\frac{\partial^2 M_{xx}}{\partial x^2} + \frac{2\partial^2 M_{xy}}{\partial x\partial y} + \frac{\partial^2 M_{yy}}{\partial y^2} + q_z(x,y) = 0 \quad (7)$$

## 2.9 Mindlin FSDPT Equations

Substituting Equations (5a) – (5c) into Equation (7) gives, after simplification:

$$D\nabla^2\left(\frac{\partial\lambda_x}{\partial x} + \frac{\partial\lambda_y}{\partial y}\right) = -q_z(x,y) \quad (8)$$

Similarly, substitution of Equations (5a), (5b) and (5d) into Equation (6a) gives:

$$k_s Gh\left(\lambda_x + \frac{\partial w}{\partial x}\right) = \frac{\partial D}{\partial x}\left(\frac{\partial\lambda_x}{\partial x} + \mu\frac{\partial\lambda_y}{\partial y}\right) + \frac{\partial}{\partial y}D(1-\mu)\left(\frac{\partial\lambda_x}{\partial y} + \frac{\partial\lambda_y}{\partial x}\right) \quad (9)$$

Simplifying,

$$\lambda_x + \frac{\partial w}{\partial x} = \frac{D}{D_s}\left(\frac{\partial^2\lambda_x}{\partial x^2} + \frac{\partial^2\lambda_x}{\partial y^2} + \frac{\partial^2\lambda_y}{\partial x\partial y} - \mu\frac{\partial^2\lambda_x}{\partial y^2}\right) \quad \ldots(10)$$

$$D_s = k_s Gh \quad (11)$$

Similarly,

$$D_s\left(\lambda_y + \frac{\partial w}{\partial y}\right) = \frac{\partial}{\partial x}D(1-\mu)\left(\frac{\partial\lambda_x}{\partial y} + \frac{\partial\lambda_y}{\partial x}\right) +$$

$$\frac{\partial}{\partial y} D\left(\mu \frac{\partial \lambda_x}{\partial x} + \frac{\partial \lambda_y}{\partial y}\right) \quad (12)$$

Simplifying,

$$\frac{D_s}{D}\left(\lambda_y + \frac{\partial w}{\partial y}\right) = \left(\frac{\partial^2 \lambda_y}{\partial x^2} + \frac{\partial^2 \lambda_y}{\partial y^2} + \frac{\partial^2 \lambda_x}{\partial x \partial y} - \mu \frac{\partial^2 \lambda_y}{\partial x^2}\right) \quad \ldots(13)$$

## 3. Double Fourier Series Method (DFSM)

For simple supports at boundaries (0, *y*), (*a*, *y*), (*x*, 0), (*x*, *b*), the boundary conditions are:

$$\begin{aligned}
&M_{xx}(0, y) = M_{xx}(a, y) = 0 \\
&\lambda_y(0, y) = \lambda_y(a, y) = 0 \\
&w(0, y) = w(a, y) = 0 \\
&M_{yy}(x, 0) = M_{yy}(x, b) = 0 \\
&\lambda_x(x, 0) = \lambda_x(x, b) = 0 \\
&w(x, y=0) = w(x, y=b) = 0
\end{aligned} \quad (14)$$

The generalized displacements are constructed using double Fourier series terms satisfying all the boundary conditions as:

$$\begin{aligned}
&w(x, y) = \sum_m^\infty \sum_n^\infty W_{mn} \sin(\bar{\alpha}_m x)\sin(\bar{\beta}_n y) \\
&\lambda_x(x, y) = \sum_m^\infty \sum_n^\infty A_{mn} \cos(\bar{\alpha}_m x)\sin(\bar{\beta}_n y) \\
&\lambda_y(x, y) = \sum_m^\infty \sum_n^\infty B_{mn} \sin(\bar{\alpha}_m x)\cos(\bar{\beta}_n y)
\end{aligned} \quad (15)$$

where $\bar{\alpha}_m = m\pi/a; \quad \bar{\beta}_n = n\pi/b$ (16)

$m = 1, 2, 3, \ldots \infty; \quad n = 1, 2, 3, \ldots \infty$

$W_{mn}$ are amplitudes of $w(x, y)$

$A_{mn}$ are amplitudes of $\lambda_x(x, y)$

$B_{mn}$ are amplitudes of $\lambda_y(x, y)$

The load $q_z(x, y)$ is represented by the double Fourier series

$$q_z(x, y) = \sum_m^\infty \sum_n^\infty q_{mn} \sin(\bar{\alpha}_m x)\sin(\bar{\beta}_n y) \quad (17)$$

$q_{mn}$ are Fourier coefficients of the load function $q_z(x, y)$

Equation (8) becomes:

$$\sum_m^\infty \sum_n^\infty \Big\{\bar{\alpha}_m\left(\bar{\alpha}_m^2 + \bar{\beta}_n^2\right) A_{mn} \sin(\bar{\alpha}_m x)\sin(\bar{\beta}_n y) + \bar{\beta}_n\left(\bar{\alpha}_m^2 + \bar{\beta}_n^2\right) B_{mn} \sin(\alpha_m x)\sin(\beta_n y)\Big\} = \frac{-1}{D}\sum_m^\infty \sum_n^\infty q_{mn} \sin(\bar{\alpha}_m x)\sin(\bar{\beta}_n y) \quad (18)$$

Hence,

$$\bar{\alpha}_m\left(\bar{\alpha}_m^2 + \bar{\beta}_n^2\right) A_{mn} + \bar{\beta}_n\left(\bar{\alpha}_m^2 + \bar{\beta}_n^2\right) B_{mn} = \frac{-q_{mn}}{D} \quad \ldots(19)$$

Similarly, Equation (10) becomes:

$$\sum_m^\infty \sum_n^\infty \Big(A_{mn} \cos(\bar{\alpha}_m x)\sin(\bar{\beta}_n y) + \alpha_m W_{mn} \cos(\bar{\alpha}_m x)\sin(\bar{\beta}_n y)\Big) = \frac{D}{D_s}\sum_m^\infty \sum_n^\infty \Big\{-\left(\bar{\alpha}_m^2 + \bar{\beta}_n^2\right) A_{mn} \cos(\bar{\alpha}_m x)\sin(\bar{\beta}_n y) - \bar{\alpha}_m \beta_n B_{mn} \cos(\bar{\alpha}_m x)\sin(\bar{\beta}_n y) + \mu\beta_n^2 A_{mn} \cos(\bar{\alpha}_m x)\sin(\bar{\beta}_n y)\Big\} \quad (20)$$

Hence,

$$A_{mn} + \alpha_m W_{mn} = \frac{D}{D_s}\Big(-(\bar{\alpha}_m^2 + \bar{\beta}_n^2) A_{mn} - \bar{\alpha}_m \bar{\beta}_n B_{mn} + \mu\beta_n^2 A_{mn}\Big) \quad (21)$$

Simplifying,

$$A_{mn} \frac{D}{D_s}\Big(-(\bar{\alpha}_m^2 + \bar{\beta}_n^2) + \mu\bar{\beta}_n^2\Big) - A_{mn} - \frac{D}{D_s}\bar{\alpha}_m \bar{\beta}_n B_{mn} - \alpha_m W_{mn} = 0 \quad (22)$$

Similarly, Equation (13) becomes:

$$\sum_m^\infty \sum_n^\infty \Big(A_{mn} \sin(\bar{\alpha}_m x)\cos(\bar{\beta}_n y) + \bar{\beta}_n W_{mn} \sin(\bar{\alpha}_m x)\cos(\bar{\beta}_n y)\Big) = \frac{D}{D_s}\sum_m^\infty \sum_n^\infty \Big\{-\left(\bar{\alpha}_m^2 + \bar{\beta}_n^2\right) B_{mn} \sin(\bar{\alpha}_m x)\cos(\bar{\beta}_n y) - \alpha_m \beta_n A_{mn} \sin(\bar{\alpha}_m x)\cos(\bar{\beta}_n y) + \mu\alpha_m^2 B_{mn} \sin(\bar{\alpha}_m x)\cos(\bar{\beta}_n y)\Big\} \quad (23)$$

Thus, simplifying,

$$\sum_m^\infty \sum_n^\infty (A_{mn} + \beta_n W_{mn}) \sin(\bar{\alpha}_m x)\cos(\bar{\beta}_n y) = \frac{D}{D_s}\sum_m^\infty \sum_n^\infty \Big(-(\bar{\alpha}_m^2 + \bar{\beta}_n^2) B_{mn} - \alpha_m \beta_n A_{mn} + \mu\alpha_m^2 B_{mn}\Big) \sin(\bar{\alpha}_m x)\cos(\bar{\beta}_n y) \quad (24)$$

Hence,

$$A_{mn} + \beta_n W_{mn} = \frac{D}{D_s}\left(-(\bar{\alpha}_m^2 + \bar{\beta}_n^2)B_{mn} - \bar{\alpha}_m \bar{\beta}_n A_{mn} + \mu\bar{\alpha}_m^2 B_{mn}\right) \quad (25)$$

Or,

$$\frac{D}{D_s} A_{mn}(-\bar{\alpha}_m \bar{\beta}_n) - A_{mn} + \frac{D}{D_s} B_{mn}\left(\mu\bar{\alpha}_m^2 - (\bar{\alpha}_m^2 + \bar{\beta}_n^2)\right) - \bar{\beta}_n W_{mn} = 0 \quad (26)$$

Using matrix format, Equations (19), (22) and (26) are expressed as Equation (27):

$$\begin{pmatrix} a_{11} & a_{12} & a_{13} \\ a_{21} & a_{22} & a_{23} \\ a_{31} & a_{32} & a_{33} \end{pmatrix} \begin{pmatrix} A_{mn} \\ B_{mn} \\ W_{mn} \end{pmatrix} = \begin{pmatrix} -\frac{q_{mn}}{D} \\ 0 \\ 0 \end{pmatrix} \quad (27)$$

where:

$$a_{11} = \bar{\alpha}_m(\bar{\alpha}_m^2 + \bar{\beta}_n^2)$$
$$a_{12} = \bar{\beta}_n(\bar{\alpha}_m^2 + \bar{\beta}_n^2)$$
$$a_{13} = 0$$
$$a_{21} = \frac{D}{D_s}\left(\mu\bar{\beta}_n^2 - (\bar{\alpha}_m^2 + \bar{\beta}_n^2)\right) - 1$$
$$a_{22} = -\frac{D}{D_s}\bar{\alpha}_m \bar{\beta}_n \quad (28)$$
$$a_{23} = -\bar{\alpha}_m$$
$$a_{31} = -\frac{D}{D_s}\bar{\alpha}_m \bar{\beta}_n - 1$$
$$a_{32} = \frac{D}{D_s}\left(\mu\bar{\alpha}_m^2 - (\bar{\alpha}_m^2 + \bar{\beta}_n^2)\right)$$
$$a_{33} = -\bar{\beta}_n$$

Using Cramer's rule, the unknown amplitudes $A_{mn}$, $B_{mn}$ and $W_{mn}$ are determined in terms of $q_{mn}$. Hence the problem is solved for known values of $q_z(x, y)$ for which $q_{mn}$ are found using Fourier series theory.

## 4. Results and Discussion

### 4.1 Uniformly distributed loads

For uniformly distributed load of intensity $q(x, y) = q_0$, the Fourier series coefficients $q_{mn}$ are expressed by:

$$q_{mn} = \frac{4q_0}{ab}\int_0^a \sin\frac{m\pi x}{a}dx \int_0^b \sin\frac{n\pi y}{b}dy \quad (29)$$

Integrating, gives:

$$q_{mn} = \frac{16q_0}{mn\pi^2}, \quad m = 1, 3, 5, \ldots \infty, \quad n = 1, 3, 5, \ldots \infty$$
$$q_{mn} = 0, \quad m = 2, 4, 6, \ldots \infty, \quad n = 2, 4, 6, \ldots \infty \quad (30)$$

### 4.2 Linearly distributed loads

The linear load distribution, $q_z(x, y) = q_0 x / a$ over $0 \le x \le a,\ 0 \le y \le b$ on the thick plate is as depicted in Figure 4.

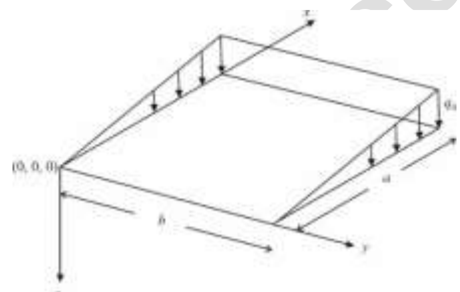


Figure 4: Isometric view of linear distribution of loading on thick rectangular plate

By the Fourier series expansion, the coefficient (of the linearly distributed load) $q_{mn}$ is expressed by:

$$q_{mn} = \frac{4}{ab}\int_0^a\int_0^b \frac{q_0 x}{a}\sin\frac{m\pi x}{a}\sin\frac{n\pi y}{b}dxdy \quad (31)$$

Evaluating the integrals gives:

$$q_{mn} = \frac{8q_0 \cos m\pi}{mn\pi^2} \quad (32)$$

where $m = 1, 3, 5, 7, \ldots \infty;\ n = 1, 3, 5, 7, \ldots \infty$

The results are presented in terms of dimensionless displacements and stresses defined in Equations (33). The results for displacements and stresses are formulated in Table 1 for the present study and for previous works. The results for linearly distributed loads are presented in Table 2 for present work and for previous studies in the literature.

Hence, $u = \bar{u}\frac{qh}{E}s^3$

$$w = \frac{\bar{w}}{100E}qhs^4 \quad (33)$$
$$\sigma_{xx} = \bar{\sigma}_{xx} q s^2$$

$\tau_{xy} = \bar{\tau}_{xy} qs, \quad \tau_{zx} = \bar{\tau}_{zx} qs$

Table 1
In-plane displacements $\bar{u}(0, 0.5b, \pm 0.5h)$, transverse displacements $\bar{w}(0.5a, 0.5b, 0)$, in-plane normal stress $\bar{\sigma}_{xx}(0.5a, 0.5b, \pm 0.5h)$, in-plane shear stress $\bar{\tau}_{xy}$ at $(0, 0, \pm 0.5h)$, shear stress $\bar{\tau}_{zx}^{CR}$, $\bar{\tau}_{zx}^{EE}$ at $(0, 0.5b, 0)$ in isotropic, square plates subjected to uniform transverse load.

| $s = \frac{a}{h}$ | Reference | Plate Models | $\bar{u}$ | $\bar{w}$ | $\bar{\sigma}_{xx}$ | $\bar{\tau}_{xy}$ | $\bar{\tau}_{zx}^{CR}$ | $\bar{\tau}_{zx}^{EE}$ |
|---|---|---|---|---|---|---|---|---|
| | Present | FSDPT | 0.074 (2.78%) | 5.633 (-1.07%) | 0.287 (-6.51%) | 0.195 | 0.330 (-31.54%) | 0.495 |
| | Reddy (2004) | HSDPT | 0.079 (9.72%) | 5.869 (3.07%) | 0.299 (-2.61%) | 0.218 | 0.482 (4.78%) | 0.452 |
| | Pagano (1970) | Elasticity (Exact) | 0.072 | 5.694 | 0.307 | – | 0.460 | – |
| | Ghugal and Sayyad (2013) | TSDPT | 0.074 (2.78%) | 5.680 (-0.25%) | 0.318 (3.58%) | 0.208 | 0.483 (5.0%) | 0.420 |
| 4 | Ghugal and Pawar (2011a) | HPSDPT | 0.079 (9.72%) | 5.858 (2.88%) | 0.297 (-3.26%) | 0.185 | 0.477 (3.70%) | 0.451 |
| | Sayyad (2013) | ESDPT | 0.079 (9.72%) | 5.816 (2.14%) | 0.300 (-2.28%) | 0.223 | 0.481 (4.57%) | 0.472 |
| | Rouzegar and Abdoli-Sharifpoor (2015) | FE-RPT | – | – | – | – | – | – |
| | Kirchhoff (1850) | CPT / KPT | 0.074 (2.78%) | 4.436 (-22.09%) | 0.287 (-6.51%) | 0.195 | – | 0.495 |
| | Present | FSDPT | 0.074 (1.37%) | 4.670 (0.65%) | 0.2873 (0.59%) | 0.1946 | 0.3928 (-19.34%) | 0.495 |
| | Reddy (2004) | HSDPT | 0.075 (2.74%) | 4.670 (0.65%) | 0.2890 (0%) | 0.1990 | 0.4890 (0.41%) | 0.486 |
| | Pagano (1970) | Elasticity (Exact) | 0.073 | 4.640 | 0.289 | – | 0.487 | – |
| | Ghugal and Sayyad (2013) | TSDPT | 0.073 (0%) | 4.625 (-0.32%) | 0.307 (6.23%) | 0.195 | 0.504 (3.49%) | 0.481 |
| 10 | Ghugal and Pawar (2011a) | HPSDPT | 0.074 (1.37%) | 4.665 (0.54%) | 0.289 (0%) | 0.193 | 0.489 (0.41%) | 0.486 |
| | Sayyad (2013) | ESDPT | 0.075 (2.74%) | 4.658 (0.39%) | 0.289 (0%) | 0.204 | 0.494 (1.44%) | 0.490 |
| | Rouzeger and Abdoli-Sharifpoor (2015) | FE-RPT | – | 4.650 (0.22%) | 0.2883 (-0.24%) | 0.1971 | 0.4718 (-3.12%) | – |
| | Kirchhoff (1850) | CPT / KPT | 0.074 (1.37%) | 4.44 (-4.31%) | 0.2873 (-0.59%) | 0.1946 | – | 0.495 |

Table 2
In-plane displacements $\bar{u}(0, 0.5b, \pm 0.5h)$, transverse displacements $\bar{w}(0.5a, 0.5b, \pm 0.5h)$, in-plane normal stress $\bar{\sigma}_{xx}(0.5a, 0.5b, \pm 0.5h)$, in-plane shear stress $\bar{\tau}_{xy}$ at $(0, 0, \pm 0.5h)$, transverse

shear stresses $\bar{\tau}_{zx}^{CR}(0, 0.5b, 0)$, $\bar{\tau}_{zx}^{EE}(0, 0.5b, 0)$ in isotropic square plates under to linear distribution of transverse loading $q(x, y) = \frac{q_0 x}{a}$

| $s = \frac{a}{h}$ | Reference | Plate Models | $\bar{u}$ | $\bar{w}$ | $\bar{\sigma}_{xx}$ | $\bar{\tau}_{xy}$ | $\bar{\tau}_{zx}^{CR}$ | $\bar{\tau}_{zx}^{EE}$ |
|---|---|---|---|---|---|---|---|---|
| | Present Results | FSDPT | 0.0370 (2.78%) | 2.817 (-1.05%) | 0.144 (-5.88%) | 0.097 | 0.165 (-28.26%) | 0.247 |
| | Reddy (2004) | HSDPT | 0.0395 (9.72%) | 2.935 (3.09%) | 0.150 (-1.96%) | 0.109 | 0.241 (4.78%) | 0.226 |
| | Pagano (1970) | Elasticity (Exact) | 0.0360 | 2.847 | 0.153 | – | 0.230 | – |
| | Ghugal and Sayyad (2013) | TSDPT | 0.0370 (2.78%) | 2.840 (-0.25%) | 0.159 (3.92%) | 0.104 | 0.241 (4.78%) | 0.210 |
| 4 | Ghugal and Pawar (2011a) | HPSDPT | 0.0395 (9.72%) | 2.929 (2.88%) | 0.148 (-3.27%) | 0.092 | 0.239 (3.91%) | 0.225 |
| | Sayyad (2013) | ESDPT | 0.0396 (10%) | 2.908 (2.14%) | 0.150 (-1.96%) | 0.111 | 0.240 (4.35%) | 0.236 |
| | Rouzegar and Abdoli-Sharifpoor (2015) | FE-RPT | – | – | – | – | – | – |
| | Kirchhoff (1850) | CPT / KPT | 0.0370 (2.78%) | 2.218 | 0.144 (-5.88%) | 0.097 | – | 0.237 |
| | Present | FSDPT | 0.0370 (1.37%) | 2.335 (0.65%) | 0.143 (-0.69%) | 0.097 | 0.165 (-32.38%) | 0.248 |
| | Reddy (2004) | HSDPT | 0.0375 (2.74%) | 2.333 (0.56%) | 0.144 (0%) | 0.101 | 0.246 (0.82%) | 0.243 |
| | Pagano (1970) | Elasticity (Exact) | 0.0365 | 2.320 | 0.144 | – | 0.244 | – |
| | Ghugal and Sayyad (2013) | TSDPT | 0.0365 (0%) | 2.313 (-0.30%) | 0.153 (6.25%) | 0.097 | 0.252 (3.28%) | 0.241 |
| 10 | Ghugal and Pawar (2011a) | HPSDPT | 0.0370 (1.37%) | 2.332 (0.52%) | 0.144 (0%) | 0.096 | 0.245 (0.41%) | 0.243 |
| | Sayyad (2013) | ESDPT | 0.0375 (2.74%) | 2.329 (0.39%) | 0.144 (0%) | 0.102 | 0.247 (1.23%) | 0.245 |
| | Rouzeger and Abdoli-Sharifpoor (2015) | FE-RPT | – | 2.3301 (0.44%) | 0.1442 (0.14%) | 0.0781 | – | – |
| | Kirchhoff (1850) | CPT / KPT | 0.0370 (1.37%) | 2.218 (-4.4%) | 0.143 (-0.69%) | 0.097 | – | 0.248 |



## 4.4 Discussion of Results

This paper has presented a rigorous first principles derivation of PDEs for flexural analysis of Mindlin's plate. The equations need shear correction factors but satisfy kinematic, constitutive and equilibrium equations.

The GDEE are a coupled system of three equations in three displacements parameters. The equations are solved using the DFSM which reduced the system to algebraic equations with unknown displacements amplitudes. Solutions were obtained for two cases of uniformly distributed loading and linearly distributed loading and illustrated in Tables 1 and 2 respectively.

Table 1 presents the in-plane displacements $\bar{u}(0, 0.5b, \pm 0.5h)$, transverse displacement $\bar{w}(0.5a, 0.5b, 0)$, in-plane stress $\bar{\sigma}_{xx}(0.5a, 0.5b, \pm 0.5h)$, in-plane shear stress $\bar{\tau}_{xy}$ at $(0, 0, \pm 0.5h)$, and transverse shear stress from constitutive relations (CR) $\bar{\tau}_{zx}^{CR}$, and $\tau_{zx}$ computed from equilibrium equations (EE) denoted by $\bar{\tau}_{zx}^{EE}$ at $(0, 0.5b, 0)$ respectively.

The results in Table 1 are presented for homogeneous, isotropic square plates under uniform loading. Table 1 also presents comparative results from previous related studies by Reddy (2004), Pagano (1970), Ghugal and Sayyad (2013), Ghugal and Pawar (2011), Sayyad (2013) and Kirchhoff (1850).

Table 1 shows that for $a/h$ = 4, the present results are closely similar with previous results obtained by using HSDPT, HPSDPT. Present results differ from the exact results of Pagano by 2.78% for $\bar{u}$, -1.07% for $\bar{w}$ and -6.51%for $\bar{\sigma}_{xx}$, for $s = a/h$ = 4. This illustrates that for $a/h$ = 4, the present results more accurately predict the values for $\bar{u}$ and $\bar{w}$ than Reddy's results which differ from the exact results by 9.72% for $\bar{u}$, and 3.07% for $\bar{w}$.

Table 1 further shows that for $a/h$ = 10, the present results differ from the exact results by 1.37% for $\bar{u}$, 0.65% for $\bar{w}$, and -0.59% for $\bar{\sigma}_{xx}$. The present results for $a/h$ = 10 are comparable to previous results that used HSDPT, TSDPT, HPSDPT, FSDPT, and FE-RPT.

Table 2 presents the in-plane displacements $\bar{u}(0, 0.5b, \pm 0.5h)$, transverse displacements $\bar{w}(0.5a, 0.5b, 0)$, in-plane stresses $\bar{\sigma}_{xx}(0.5a, 0.5b, \pm 0.5h)$, in-plane shear stress at $\tau_{xy}(0, 0, \pm 0.5h)$, and transverse shear stresses $\tau_{zx}^{CR}, \tau_{zx}^{EE}$ at $(0, 0.5b, 0)$ respectively.

The results in Table 2 are presented for homogeneous, isotropic square plate under to linear distribution of loading. It further presents comparative results from previous related studies by Reddy (2004), Pagano (1970), Ghugal and Sayyad (2013), Ghugal and Pawar (2011), Sayyad (2013) and Kirchhoff (1850).

Table 2 illustrates that for $s = a/h = 4$ and $s = a/h = 10$, the present results are closely similar to previous results obtained using HSDPT, TSDPT, HPSDPT, ESDPT and elasticity methods. For $a/h$ = 4 the present results differ from the exact elasticity results of Pagano (1970) by 2.78% for $\bar{u}$, -1.05% for $\bar{w}$, -5.88% for $\bar{\sigma}_{xx}$. The differences of the present results are comparable to the differences obtained using HSDPT, TSDPT, HPSDPT, ESDPT For $a/h$ = 10, the present results differ from the exact results by 1.37% for $\bar{u}$, 0.65% for $\bar{w}$, and -0.69% for $\bar{\sigma}_{xx}$. The results are comparable to previous results by Reddy (2004), Ghugal and Sayyad (2013), Ghugal and Pawar (2011), Sayyad (2013) and Rouzeger and Abdoli-Sharifpoor (2015).

## 5. Conclusion

The study has presented a detailed rigorous first principles derivation of Mindlin plate bending formulation. It incorporates transverse shear stress correction factors, and violates shearing stress-free boundary conditions at top and bottom surfaces $(z = \pm 0.5h)$. In conclusion:

(i) Mindlin's plate bending problem satisfies kinematic relations, constitutive laws and equilibrium equations; and is considered exact within the framing of the underlying hypotheses of small displacement elasticity theories for homogenous isotropic thick plates.

(ii) the formulation was done using the equilibrium approach.

(iii) the present results for inplane displacements and transverse displacement for uniformly distributed transverse loads are comparable to results previously obtained using

HSDPT, HPSDPT, ESDPT and TSDPT.

(iv) the present results for inplane normal stresses and inplane shear stresses for linearly distributed loadings are also comparable with previous solutions that used HSDPT, HPSDPT, ESDPT and TSDPT.

(v) The present results violate transverse shear stress free boundary conditions, do not accurately predict the transverse shear stress obtained by constitutive relations ($\tau_{zx}^{CR}$). The $\tau_{zx}^{CR}$ for uniformly distributed load obtained by the present study is -31.54% different from the exact results for $a/h$ = 4 and -19.34% different for $a/h$ = 10. This is because the FSDPT violates the transverse shear stress-free boundary conditions at the plate's top and bottom surfaces $(x, y, \pm 0.5h)$

(vi) For the case of linear distribution of loading $\tau_{zx}^{CR}$ from this present study is -28.26% different from exact solutions for $ah^{-1}$ = 4; and -32.38% different from the exact solution for $ah^{-1}$ = 10. This is because the present FSDPT is in violation of the shear stress-free boundary conditions at both top and bottom surfaces $z = \pm 0.5h$

## References


Alcybeev, G.O., Goloskokov, D.P. and Matrosov, A.V. (2022). "The superposition method in the problem of a thin isotropic plate clamped along the contour," *Vestnik of Saint Petersburg University. Applied Mathematics Computer Sciences, Control Processes*, 18(3), 347 – 364. https://doi.org/10.21638/11701/spbu10.2022.305

Altekin M. (2018) "Bending of super-elliptical Mindlin plates by finite element method Teknik Dergi 2018, 8469-8496.

Belounar A, Benmebarek S., and Belounar L. (2020) "Strain based triangular finite element for plate bending analysis" Mechanics of Advanced Materials and Structures 27(8), 620-632 https://doi.org/10.1080/15376494.2018.1488310

Do, V.T., Pham, V.V. and Nguyen, H.N. (2020). "On the development of refined plate theory for static bending behavior of functionally graded plates," *Mathematical Problems in Engineering*, 2020, 2836763, 13pages. https://doi.org/10.1155/2020/2836763

Gajbhiye, P.D., Bhaiya, V. and Ghugal, Y.M. (2021). "Free vibration analysis of thick isotropic plate using 5th order shear deformation theory," *Progress in Civil and Structural Engineering*, 1(1), 1 – 11. https://doi.org/10.38202/pcse.v1i1.2

Gajbhiye, P.D., Bhaiya, V. and Ghugal, Y.M. (2022). "Bending analysis of sandwich plates subjected to various mechanical loadings using quasi-three-dimensional theory," *Journal of Aerospace Engineering*, 35(4), 04022030.

Ghugal, Y.M. and Pawar, M.D. (2011). "Flexural analysis of thick plates by hyperbolic shear deformation theory," *Journal of Experimental and Applied Mechanics*, 2(1), 1 – 21.

Ghugal, Y.M. and Sayyad, A.S. (2013). "Static flexure of thick orthotropic plates using trigonometric shear deformation theory," *Journal of Structural Engineering*, 39(5), 512 – 521.

Goloskokov, D.P. and Matrosov, A.V. (2022). "Bending of clamped orthotropic thin plates: polynomial solution," *Mathematics and Mechanics of Solids*, 27(11), 2498 – 2509, 2022.

Haggblad B., Bathe K.J. (1990) "Specifications of boundary conditions for Reissner/Mindlin plate bending finite elements" *International Journal for Numerical Methods in Engineering*, 30, 981-1011.

Ike, C.C. (2022). "Generalized integral transform method for bending analysis of clamped rectangular thin plates," *Journal of Computational Applied Mechanics*, 53(4), 599 – 625.

DOI:10.22059/JCAMECH.2022.350620.768
Ike, C.C. (2023). "A third-order shear deformation plate bending formulation for thick plates: first principles derivation and applications," *Mathematical Models in Engineering*, 9(4), 144 – 168. https://doi.org/w.21595/mme.2023.23.688
Kianmofrad F., Ghafoori E., Motavalli M., Rahimian M. (2018). "Analytical solutions for the flexural behavior of metal beams strengthened with prestressed unbonded CFRP plate," *Civil Engineering Infrastructures Journal*, 51(1), 101 – 118. https://doi.org/10.22059/CEIJ/02018.01.006
Kirchhoff, G.R. (1850). "Uber das Gleichgewicht und Bewegung einer elastischen scheibe," *Journal fur die reine und angewandte Mathematik*, 40, 85 – 88.
Mama, B.O., Oguaghamba, O.A. and Ike, C.C. (2020). "Single finite Fourier sine integral transform method for the flexural analysis of rectangular Kirchhoff plate with opposite edges simply supported, other edges clamped for the case of triangular load distribution," *International Journal of Engineering Research and Technology*, 13(7), 1802 – 1813.
Mindlin, R.D. (1951). "Influence of rotary inertia and shear on flexural motions of isotropic elastic plates," *Journal of Applied Mechanics*, 18(1), 31 – 38.
Nwoji, C.U., Mama, B.O., Onah, H.N. and Ike, C.C. (2018). "Flexural analysis of simply supported rectangular Mindlin plates under bisinusoidal transverse load," *ARPN Journal of Engineering and Applied Sciences*, 13(15), 4480 – 4488.
Onah, H.N., Onyia, M.E., Mama, B.O., Nwoji, C.U. and Ike, C.C. (2020). "First principles derivation of displacement and stress functions for three dimensional elastostatic problems, and application to the flexural analysis of thick circular plates," *Journal of Computational Applied Mechanics*, 51(1), 184 – 198. https://doi.org/10.22059/jcamech.2020.295989.471
Onyeka, F.C., Okeke, T.E. and Mama, B.O. (2022). "Static elastic bending analysis of a three dimensional clamped thick rectangular plate using energy method," *HighTech and Innovation Journal*, 3(3), 267 – 281. DOI:10.28991/HIJ-2022-03-03-03
Onyeka, F.C., Nwa-David, C.D and Mama, B.O. (2023). "Static bending solutions for an isotropic rectangular clamped/simply supported plate using 3-D plate theory," *Journal of Computational Applied Mechanics*, 54(1), 1 – 18. DOI:10.22059/JCAMECH.2022.349835.764
Pagano, N.J. (1970). "Exact solutions for bi-directional composite and sandwich plates," *Journal of Composite Materials*, 4, 20 – 34.
Pisacic, K., Horvat, M. and Botak, Z. (2019). "Finite difference solution of plate bending using Wolfram Mathematica," *Technicki Glasnik*, 13(3), 241 – 247. https://doi.org/10.31803/tg_2019.0328111708
Reddy, J.N. (2004). *Mechanics of Laminated and Composite Plates and Shell Theory and Applications*, 2nd Edition, CRC Press, Boca Raton FL.
Rouzegar, J. and Abdoli-Sharifpoor, R. (2015). "A finite element formulation for bending analysis of isotropic and orthotropic plates based on two-variable refined plate theory," *Scientia Iranica Transactions B Mechanical Engineering*, 22(1), 196 – 207.
Sayyad, A.S. (2013). "Flexure of thick orthotropic plates by exponential shear deformation theory," *Latin American Journal of Solids and Structures*, 10, 473 – 490.
Shahnavaz F., Attarnejad R., Shaloudegi K., Firouzjaei R.K. (2023). "Innovative efficient element for analysis of FGM plates using FEM," *Civil Engineering and Infrastructures Journal*, 56(1), 205 – 219. https://doi.org/10.22059/CEIJ/2022.318133.1739
Shetty R.A., Deepak S.A., Sudheer K.K., Dushyanthkumar G.L (2022) "Thick plate bending analysis using a single variable simple plate theory" Materials Today Proceedings 54 (2), 191 – 195 https://doi.org/10.1016/jmatp2021/.08.289
Singhatandgid, P. and Singhanart, T. (2019). "The Kantorovich method applied to the

bending, buckling, vibration and 3D stress analysis of plates: a literature review," *Mechanics of Advanced Materials and Structures*, 26(2), 170 – 188.

Yekani, S.M.A, Fallah F. (2020) "A Levy solution for bending, buckling and vibration of Mindlin micro plates with a modified couple stress theory," *SN Applied Sciences*, 2, 2169, htts://doi.org/10.1007/s42452-020-03939-w

Zhong Y., Xu, Q. (2017) "Analysis bending solutions of clamped rectangular thick plate" Mathematical Problems in Engineering 2017 (7), 7539276 https://doi.org/10.1155/2017/7539276